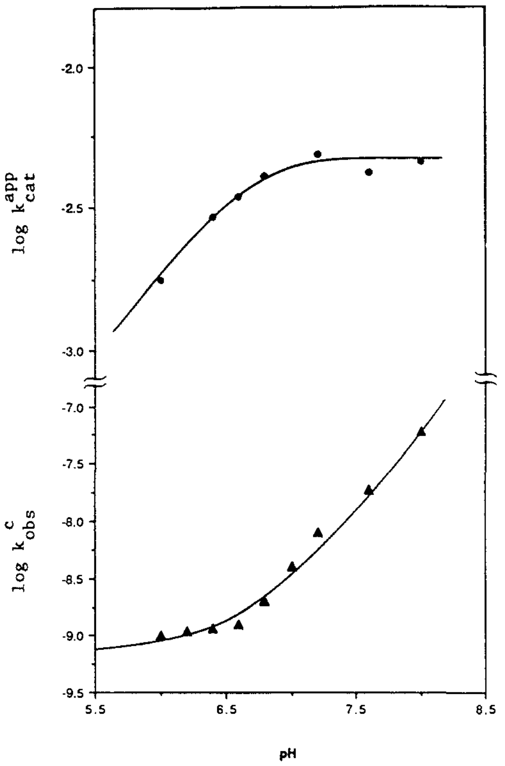

Figure 2. log k_{cat}^{app} vs pH plot (●) of antibody (30C6) catalyzed reaction of 3. The calculated line was obtained by using $k_{cat}^{app} = k_{cat}[K_a/(K_a + a_H)]$. log k_{obsd}^{c} vs pH (▲) of 3 extrapolated to zero buffer concentration. The calculated line was obtained by using $k_{obsd}^{c} = k_0 + k_{OH^-}[OH^-]$. Values for k_{cat}, K_a, k_0, and k_{OH^-} are listed in the text.

The initial rate of hydrolysis of **3** (50 mM phosphate, 100 mM NaCl, pH 7.2, 37 °C) catalyzed by 30C6 (20 μM) followed Michaelis-Menten kinetics[10] with values of k_{cat}^{app} and K_m of (5 ± 0.2) × 10^{-3} min^{-1} and 1.12 ± 0.05 mM, respectively. The antibody-catalyzed hydrolysis of benzoate **3** was competitively inhibited (K_i = 83 ± 5 μM) by the addition of pyridinium salt **1b**. The pH dependence of the hydrolysis of **3** was examined in the presence of 30C6 (20 μM) between pH 6.0 and 7.2 (Bis-tris) and pH 7.2 and 8.0 (phosphate), both at 50 mM buffer and 100 mM NaCl, 37 °C (Figure 2). The pH dependence of k_{cat}^{app} reveals participation by the basic form of a dissociable group, whose pK_a was determined to be 6.26 ± 0.05 (Figure 2). Variation of the buffer ion concentration (12.5–50 mM) showed no dependency on k_{cat} on the presence of buffer species. For direct comparison, we measured the rates of hydrolysis (k_{obsd}^{c}) of **3** over the idential pH region extrapolated to zero buffer concentration (Figure 2). The pH rate profile implicated the species[11] involved in cleavage to be water in the pH region of 6.0–6.5 (k_0 = 0.6 × 10^{-9} min^{-1}) and hydroxide from pH 6.6 and above (k_{OH^-} = 4.2 × 10^{-2} min^{-1}). The ratio of k_{cat}/k_0, a comparison of the pH-independent antibody-catalyzed rate of **3** to that in water, corresponds to a rate acceleration by the antibody of over 1,000,000-fold. *Significantly, the pH optimum of the antibody-catalyzed reaction has been moved into the neutral pH region* by participation by as yet an unidentified amino acid.

We foresee an ensemble of multiple charges which might produce a number of catalytic groups giving us an additive rate effect. This possibility combined with access to a much larger repertoire of potential catalytic antibodies[12] improves the probability of developing superior catalysts.

---

(10) Concentrations of **4** were determined by HPLC measurements of its peak height relative to that of an internal standard over 1–2 h (three or more determinations). A standard curve showed linearity with concentrations of **4** up to 0.5 mM.

(11) Bruice, T.; Benkovic, S. *Bioorganic Chemistry*; Benjamin: New York, 1965; Vol. 1.

(12) Sastry, L.; Alting-Mees, M.; Huse, W. D.; Short, J. M.; Sorge, J. A.; Hay, B. N.; Janda, K. D.; Benkovic, S. J.; Lerner, R. A. *Proc. Natl. Acad. Sci. U.S.A.* **1989**, *86*, 5728.

Simple and Accurate Determination of Ion Translational Energy in Ion Cyclotron Resonance Mass Spectroscopy

Peter B. Grosshans,[†] Patrick Shields,[‡] and
Alan G. Marshall*,[†,§]

Departments of Chemistry, Biochemistry, and Physics
The Ohio State University
120 West 18th Avenue, Columbus, Ohio 43210

Received September 21, 1989

Fourier transform ion cyclotron resonance (FT/ICR) mass spectrometry is the most versatile and widely used technique for analysis of gas-phase ion/molecule reaction pathways, kinetics, equilibria, and energetics and is also suitable for a wide range of analytical applications, as summarized in numerous recent reviews.[1-12] A powerful tool in such studies is the collision-induced dissociation (CID, also known as CAD, collision-activated dissociation) technique, in which ions are first accelerated to higher translational energy (in this case, by increase in ICR orbital radius in an ICR ion trap);[8,13] subsequent ion-neutral collisions (e.g., with Ar atoms) then result in fragmentation of the parent ion to give daughter ions. The structure of the parent ion may then be inferred from the masses of the daughter ions[14,15] and/or the neutral fragments lost.[15] From the *radius r*, of that ICR orbit, the ion orbital translational *energy* is readily found:[16]

$$\mathrm{KE} = \frac{q^2 B_0^{\,2} r^2}{2m} \qquad \text{(SI units)} \qquad (1)$$

in which q is ionic charge, m is ionic mass, and B_0 is the applied magnetic field strength. For example, the energy threshold for collision-induced dissociation may be determined from eq 1 by increasing the ICR radius (and thus ion translational energy) until the desired collision-induced dissociation is observed.[8,13]

Up to now, the translational energy of the accelerated ions in such experiments was computed from the measured radio-frequency (rf) excitation voltage amplitude and duration. Unfortunately, the equation on which all such prior computations have been based is valid only for electrodes of *infinte* extent[17] and

---

[†] Department of Chemistry.

[‡] Department of Physics.

[§] Department of Biochemistry.

(1) Marshall, A. G. *Acc. Chem. Res.* **1985**, *18*, 316–322.

(2) Marshall, A. G. *Adv. Mass Spectrom.* **1989**, *11A*, 651–669.

(3) Wilkins, C. L.; Chowdhur, A. K.; Nuwaysir, L. M.; Coates, M. L. *Mass Spectrom. Rev.* **1989**, *8*, 67–92.

(4) Cody, R. B.; Bjarnason, A.; Weil, D. A. In *Lasers in Mass Spectrometry*; Lubman, D. M., Ed.; Oxford U. Press: New York, in press.

(5) Sharpe, P.; Richardson, D. E. *Coord. Chem. Rev.* **1989**, *93*, 59–85.

(6) Freiser, B. S. In *Techniques for the Study of Ion Molecule Reactions*; Farrar, J. M., Saunders, W. H., Jr., Eds.; Wiley: New York, 1988; Vol. 20, Chapter 2, pp 61–118.

(7) Hanson, C. D.; Kerley, E. L.; Russell, D. H. In *Treatise on Analytical Chemistry*, 2nd Ed.; Wiley: New York, 1988; Vol. 11, Chapter 2.

(8) Nibbering, N. M. M. *Adv. Phys. Org. Chem.* **1988**, *24*, 1–55.

(9) Asamoto, B. *Spectroscopy* **1988**, *3*, 38–46.

(10) Buchanan, M. V.; Comisarow, M. B. In *Fourier Transform Mass Spectrometry: Evolution, Innovation, and Applications*; Buchanan, M. V., Ed.; ACS Symposium Series 359; American Chemical Society: Washington, DC, 1987; pp 1–20.

(11) Gross, M. L.; Rempel, D. L. *Science* **1984**, *226*, 261–268.

(12) Wanczek, K.-P. *Int. J. Mass Spectrom. Ion Processes* **1989**, *95*, 1–38.

(13) Freiser, B. S. *Talanta* **1985**, *32*, 697–708.

(14) Cody, R. B. *Anal. Chem.* **1988**, *60*, 917–923.

(15) Busch, K. L.; Glish, G. L.; McLuckey, S. A. *Mass Spectrometry/Mass Spectrometry: Techniques and Applications of Tandem Mass Spectrometry*; VCH Publishers: New York, 1988.

(16) Marshall, A. G.; Verdun, F. R. *Fourier Transforms in NMR, Optical, and Mass Spectrometry: A User's Handbook*; Elsevier: Amsterdam, 1989; Chapter 7.

0002-7863/90/1512-1275$02.50/0

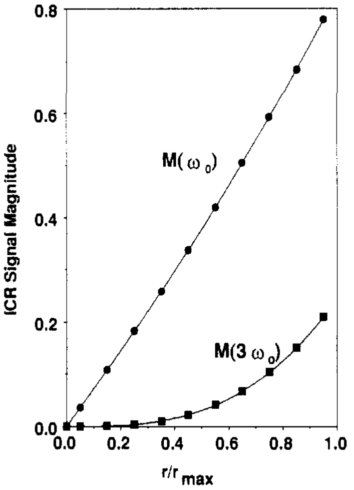

Figure 1. Theoretical FT/ICR detected signal magnitude [●, $M(\omega_0)$; ■, $M(3\omega_0)$] vs ICR orbital radius, r, computed for ions at $r = 0.05r_{\max}$, $0.15r_{\max}$, $0.25r_{\max}$, ..., $0.95r_{\max}$, in a cubic trap measuring $2r_{\max}$ on each side. The vertical axis is scaled such that the sum of the Fourier coefficients of all of the harmonics approaches 1.00 as $r \rightarrow r_{\max}$. Note that the "third harmonic" signal at frequency $3\omega_0$ increases faster with radius than does the signal at the "fundamental" (or "first harmonic") frequency, ω_0 (see text and Figure 2).

substantially overestimates ion radius and energy (e.g., by about 39% and 93% for a cubic trap).[18] Moreover, the error is a function of ion trap shape and ion excitation conditions [single frequency[19,20] vs frequency sweep[21,22] vs stored waveform (SWIFT),[23] etc.] and is thus not easily computed in practice.

In work to be reported fully elsewhere,[24] we have computed analytically the detected ICR signal for ion traps of *finite* dimensions and various shapes [i.e., circular or square cross section, with arbitrary length-to-width ("aspect") ratio]. As the ICR orbital radius increases, there is a nearly linear increase in the ICR signal detected at the "fundamental" orbital cyclotron frequency, $\omega_0 \cong qB_0/m$ (see Figure 1). In addition, there is an even faster nonlinear increase in the magnitude of new signals at odd-integer multiples of ω_0: namely, $3\omega_0$ (see Figure 1), $5\omega_0$, $7\omega_0$, etc.

A simple and striking consequence of this behavior is that the *ratio*, $M(3\omega_0)/M(\omega_0)$, of the magnitudes of the peaks at $3\omega_0$ and ω_0 varies *monotonically* with ICR orbital radius, as shown in Figure 2 for cubic[25] and cylindrical[26] ion traps.[27] Thus, a simple measurement of the peak magnitude ratio from Figure 2 provides an *absolute* measure of ICR orbital radius (and thus ion translational energy), *without any need to know the excitation conditions that placed the ion at that radius*. Thus, ion cyclotron orbital radius (and energy) may now be determined simply and easily from a *single* experimental measurement.

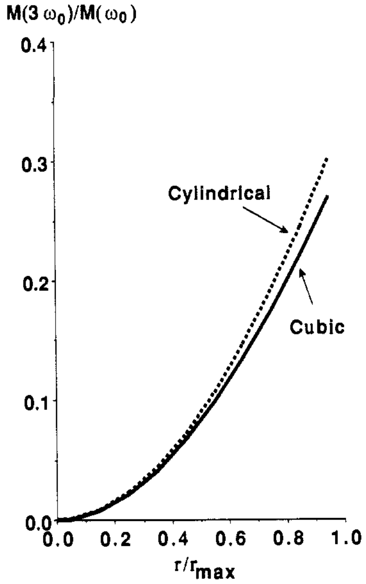

Figure 2. Theoretical ratio, $M(3\omega_0)/M(\omega_0)$, of the magnitudes of the peaks at $3\omega_0$ and ω_0 as a function of ICR orbital radius, r, for ions whose (circular) ion cyclotron orbits are centered at the geometric center of a cubic or cylindrical (length = diameter) ion trap. This graph can be used to determine the ICR orbital radius (and thus ion orbital translation energy from eq 1) directly from experimental FT/ICR magnitude-mode peak height ratio, without any knowledge of the excitation conditions that placed the ions in that orbit (see text).

The ICR orbital radius and/or energy determination made available by Figure 2 have several obvious important uses. First, it should now be possible to determine the energy of translationally excited ions in CID experiments, as noted above. Second, the ICR orbital radius determined from Figure 2 may be compared to the radius calculated from experimentally measured radio-frequency excitation voltage magnitude and duration, based on recently derived analytic expressions.[18] Thus, it should be possible to characterize quantitatively longitudinal excitation and/or "z-ejection"[26,28-31] resulting from inhomogeneous radio-frequency electric-field excitation. For example, experiments in progress[24] establish that a *distribution* in ICR orbital radii can result from differential initial or excited z-oscillation magnitude. Third, plots such as those in Figure 2 may be used to compare the calculated and actual ICR orbital radius resulting from excitation in ion traps for which the static[32] or rf[33,34] electric fields have been shimmed by segmentation[35-37] and/or addition of grounded[32] or charged[33,34] electrodes. Finally, by measuring ICR orbital radius (from Figure 2) as a function of the time delay between excitation and detection,

---

(17) Comisarow, M. B. *J. Chem. Phys.* **1978**, *69*, 4097-4104.

(18) Grosshans, P. B.; Marshall, A. G. 37th American Society for Mass Spectrometry Annual Conference on Mass Spectrometry & Allied Topics, Miami Beach, FL, May 1989; pp 1230-1231.

(19) Comisarow, M. B.; Marshall, A. G. *Chem. Phys. Lett.* **1974**, *25*, 282-283.

(20) McIver, R. T., Jr.; Hunter, R. L.; Baykut, G. *Anal. Chem.* **1989**, *61*, 489-491.

(21) Comisarow, M. B.; Marshall, A. G. *Chem. Phys. Lett.* **1974**, *26*, 489-490.

(22) Marshall, A. G.; Roe, D. C. *J. Chem. Phys.* **1980**, *73*, 1581-1590.

(23) Marshall, A. G.; Wang, T.-C.L.; Chen, L.; Ricca, T. L. *ACS Symp. Ser.* **1987**, *No. 359*, 21-33.

(24) Grosshans, P. B.; Shields, P.; Marshall, A. G., to be published.

(25) Comisarow, M. B. *Adv. Mass Spectrom.* **1980**, *8*, 1698-1706. Comisarow, M. B. *Int. J. Mass Spectrom. Ion Processes* **1981**, *37*, 251-257.

(26) Lee, S.-H.; Wanczek, K.-P.; Hartmann, H. *Adv. Mass Spectrom.* **1980**, *8B*, 1645. Nikolaev, E. N.; Gorshkov, M. V. *Int. J. Mass Spectrom. Ion Processes* **1985**, *64*, 115.

(27) This result is a direct consequence of the *finite* electrode dimensions. Prior treatment of a rectangular trap fails to predict the presence of signals at odd multiples of the fundamental frequency.[17] Prior treatment of an infinitely long line charge orbiting the axis of an infinitely long cylindrical trap correctly predicts the presence of odd harmonics,[26] but not their correct relative magnitudes in a finite cylindrical trap.

(28) Kofel, P.; Allemann, M.; Kellerhals, Hp.; Wanczek, K.-P. *Int. J. Mass Spectrom. Ion Processes* **1986**, *74*, 1-12.

(29) Rempel, D. L.; Huang, S. K.; Gross, M. L. *Int. J. Mass Spectrom. Ion Processes* **1986**, *70*, 1-184.

(30) Huang, S. K.; Rempel, D. L.; Gross, M. L. *Int. J. Mass Spectrom. Ion Processes* **1986**, *72*, 1-31.

(31) van der Hart, W. J.; van de Guchte, W. J. *Int. J. Mass Spectrom. Ion Processes* **1988**, *82*, 17-31.

(32) Wang, M.; Marshall, A. G. *Anal. Chem.* **1989**, *61*, 1288-1293.

(33) Wang, M.; Marshall, A. G. 37th American Society for Mass Spectrometry Annual Conference on Mass Spectrometry & Allied Topics, Miami Beach, FL, May 1989; pp 1226-1227.

(34) Hanson, C. D.; Kerley, E. L.; Castro, M. E.; Russell, D. H. 37th American Society for Mass Spectrometry Annual Conference on Mass Spectrometry & Allied Topics, Miami Beach, FL, May 1989; pp 1274-1275.

(35) Grosshans, P. B.; Wang, M.; Marshall, A. G. 36th American Society for Mass Spectrometry Annual Conference on Mass Spectrometry & Allied Topics, San Francisco, CA, June 1988; pp 592-593.

(36) Yang, S. S.; Rempel, D. L.; Gross, M. L. 36th American Society for Mass Spectrometry Annual Conference on Mass Spectrometry & Allied Topics, San Francisco, CA, June 1988; pp 586-587.

(37) Naito, Y.; Inoue, M. 36th American Society for Mass Spectrometry Annual Conference on Mass Spectrometry & Allied Topics, San Francisco, CA, June 1988; pp 608-609.

one may test directly various models for ICR signal damping (e.g., phase randomization vs frictional damping).[38]

The present results are quite general. The shape and position of the smooth curves in Figure 2 depend on ion trap cross-sectional shape (e.g., square or circular) and aspect ratio, but a given curve has the same shape for any size trap of a given shape, as will be described in detail elsewhere.[24]

Acknowledgment. We thank K.-P. Wanczek for private communication of his unpublished results on harmonic signals in a cylindrical ion trap. This work was supported by the NSF (CHE-8721498) and The Ohio State University.

---

(38) Comisarow, M. B. in *Ion Cyclotron Resonance Spectrometry II*; Hartmann, H., Wanczek, K.-P., Eds.; Springer-Verlag: Berlin, 1982; pp 484–513.

Photoionization (λ = 248 or 308 nm) of Triphenylmethyl Radical in Aqueous Solution. Formation of Triphenylmethyl Carbocation

J. L. Faria and S. Steenken*

Max-Planck-Institut für Strahlenchemie
D-4330 Mülheim, Federal Republic of Germany

Received September 25, 1989

Short-lived carbocations have recently become accessible for study in nucleophilic environments, due to the development and application of fast-response radiation-chemical and photochemical methods. These involve four different types of cation production: (1) formation of a radical $R^\bullet$ followed by its one-electron oxidation with metal ions,[1,2] (2) photoheterolysis of RX,[3-10] (3) photoprotonation of a C=C double bond,[8,11] and (4) heterolysis of *radical* cations to give radicals and cations.[12,13] Concerning the radical oxidation method (1),[1,2] its obvious attractiveness lies in the fact that an enormously large number of radicals of the most diverse nature can be selectively produced by photochemical and, particularly, by radiation-chemical methods,[14] making the corresponding carbocations accessible after one-electron oxidation. However, an intrinsic drawback is that one-electron oxidation of the radical $R^\bullet$ to give the cation R^+ is a *bi*molecular process, the rate of which depends on the concentration of oxidant. In practice, the concentration of oxidant is often limited to ~1 mM, which means that, if the rate *constant* for oxidation of $R^\bullet$ is 10^9–10^{10} M^{-1} s^{-1} (i.e., diffusion control), the *rate* of R^+ formation is ~ 10^6–10^7 s^{-1}. Cations with lifetimes <100 ns can therefore not be studied with this method. A faster method of converting $R^\bullet$ into R^+ is therefore desirable, and it is in this respect that photoionization of $R^\bullet$ is an attractive possibility.

Aqueous solutions containing 0.4 mM triphenylacetic acid at pH 7–10, where the carboxyl group is ionized, were photolyzed with 20-ns pulses (10–100 mJ) of 248-nm light from a Lambda Physik EMG103MSC excimer laser, and the time-dependent optical and conductance changes were recorded with Tektronix 7612 and 7912 transient recorders interfaced with a DEC LSI 11/73$^+$ computer, which also controlled the other functions of the instrument and performed on-line analysis of the experimental data.[15] As shown in Figure 1 (triangles), the photolysis leads to depletion of the parent (at 235 nm), to production of the triphenylmethyl radical (with its characteristic peak at 336 nm[16]), and to the hydrated electron, e_{aq}^- (which causes the broad band with λ(max) at 720 nm[17]). In agreement with this assignment, the 720-nm band (triangles) can be removed by admitting typical e_{aq}^- scavengers such as O_2, N_2O, or halogenated hydrocarbons such as CH_2Cl_2 or $HOCH_2CH_2Cl$ to the aqueous solutions (see Figure 1 (circles)). For $HOCH_2CH_2Cl$, the rate constant for reaction with e_{aq}^- was determined as 4.2×10^8 M^{-1} s^{-1},[18] in agreement with literature values.[19]

The yield of $Ph_3C^\bullet$ and of e_{aq}^- increases with the *square* of the incident laser power, varied in the range 0–40 mJ/pulse, which means that the production of $Ph_3C^\bullet$ and e_{aq}^- from $Ph_3CCO_2^-$ requires *two* photons (eq 1a). $Ph_3C^\bullet$ could be generated biphotonically also from Ph_3CH (eq 1b) or by reaction of Ph_3CH or $Ph_3CCO_2^-$ with photochemically (eq 2a) or radiation-chemically (eq 2b) produced $SO_4^{\bullet-}$, eq 3, indicating that the common precursor is the radical cation. Rapid decarboxylation or deprotonation of one-electron-oxidized phenylacetic acid and toluene derivatives is well documented.[20]

$$Ph_3CCO_2^- \xrightarrow[248\ nm]{h\nu} Ph_3CCO_2^{-*} \xrightarrow[248\ nm]{h\nu} Ph_3C^\bullet + CO_2 + e_{aq}^- \qquad (1a)$$

$$Ph_3CH \xrightarrow[248\ nm]{h\nu} Ph_3CH^* \xrightarrow[248\ nm]{h\nu} Ph_3C^\bullet + H^+ + e_{aq}^- \qquad (1b)$$

$$S_2O_8^{2-} \xrightarrow[248\ nm]{\overset{a}{h\nu}} 2SO_4^{\bullet-};\ S_2O_8^{2-} + e_{aq}^- \xrightarrow{b} SO_4^{2-} + SO_4^{\bullet-} \qquad (2)$$

$$Ph_3CR \xrightarrow[or\ 2h\nu/-e^-]{SO_4^{\bullet-}/-SO_4^{2-}} Ph_3CR^{\bullet+} \rightarrow Ph_3C^\bullet + R^+;\ R = H, CO_2^- \qquad (3)$$

As seen in inset b of Figure 1, $Ph_3C^\bullet$ produced by biphotonic ionization of $Ph_3CCO_2^-$ is quite long-lived (it decays bimolecularly on a longer time scale). After a few microseconds (typically 1–8 μs), the solution was subjected to a second 20-ns laser pulse[21] either

---

(1) Steenken, S.; Buschek, J.; McClelland, R. A. *J. Am. Chem. Soc.* **1986**, *108*, 2808.

(2) McClelland, R. A.; Steenken, S. *J. Am. Chem. Soc.* **1988**, *110*, 5860.

(3) Ivanov, V. B.; Ivanov, V. L.; Kuzmin, M. G. *Mol. Photochem.* **1974**, *6*, 125.

(4) Kobayashi, S.; Kitamura, T.; Taniguchi, H.; Schnabel, W. *Chem. Lett.* **1983**, 1117. Kobayashi, S.; Zhu, Q. Q.; Schnabel, W. *Z. Naturforsch.* **1988**, *43b*, 825.

(5) Van Ginkel, F. I. M.; Visser, R. J.; Varma, C. A. G. O.; Lodder, G. *J. Photochem.* **1985**, *30*, 453.

(6) Wan, P.; Yates, K.; Boyd, M. K. *J. Org. Chem.* **1985**, *50*, 2881.

(7) McClelland, R. A.; Banait, N.; Steenken, S. *J. Am. Chem. Soc.* **1986**, *108*, 7023.

(8) McClelland, R. A.; Kanagasabapathy, V. M.; Steenken, S. *Ibid.* **1988**, *110*, 6913.

(9) McClelland, R. A.; Banait, N.; Steenken, S. *Ibid.* **1989**, *111*, 2929.

(10) McClelland, R. A.; Kanagasabapathy, V. M.; Banait, N. S.; Steenken, S. *Ibid.* **1989**, *111*, 3966.

(11) Wan, P.; Yates, K. *Rev. Chem. Intermed.* **1984**, *5*, 157.

(12) Steenken, S.; McClelland, R. A. *J. Am. Chem. Soc.* **1989**, *111*, 4967.

(13) The radical cation fragmentation method was pioneered by Dorfman, who however used it (with organometallics as substrates) in nonnucleophilic and non-ionizing solvents: Dorfman, L. M.; Sujdak, R. J.; Bockrath, B. *Acc. Chem. Res.* **1976**, *9*, 352.

(14) For reviews, see, e.g.: Henglein, A.; Schnabel, W.; Wendenburg, J. *Einführung in die Strahlenchemie*; Verlag Chemie: Weinheim, 1969. Spinks, J. W. T.; Woods, R. J. *An Introduction to Radiation Chemistry*; Wiley: New York, 1976. Neta, P. *Adv. Phys. Org. Chem.* **1976**, *12*, 2. Swallow, A. J. *Prog. React. Kinet.* **1978**, *9*, 195. Butler, J.; Hoey, B. M.; Swallow, A. J. *Radiation Chemistry*; *J. Chem. Soc.*, Annual Reports C.; London, 1986; p 129 and earlier reports in this series. Farhataziz, Rodgers, M. A. J., Eds.; *Radiation Chemistry. Principles and Applications*; Verlag Chemie: Weinheim, 1987.

(15) Trinoga, R.; Reikowski, F.; Lenk, H.; Steenken, S., to be published.

(16) Taub, I. A.; Harter, D. A.; Sauer, M. C.; Dorfman, L. M. *J. Chem. Phys.* **1964**, *41*, 979.

(17) Hug, G. L. *Natl. Stand. Ref. Data Ser.* **1981**, *69*, 6.

(18) $k(e_{aq}^- + HOCH_2CH_2Cl)$ was determined as 4.8×10^8 M^{-1} s^{-1} by using e_{aq}^- produced from the 248-nm photolysis of KI.

(19) Buxton, G. V.; Greenstock, C. L.; Helman, W. P.; Ross, A. B. *J. Phys. Chem. Ref. Data* **1988**, *17*, 513.

(20) Norman, R. O. C.; Storey, P. M. *J. Chem. Soc. B* **1970**, 1099. Gilbert, B. C.; Scarratt, C. J.; Thomas, C. B.; Young, J. *J. Chem. Soc., Perkin Trans. 2* **1987**, 371. See also ref 12 and references therein.

(21) For information on the technique of "tandem" laser experiments, see, e.g.: Mehnert, R.; Brede, O.; Helmstreit, W. *Z. Chem.* **1975**, *15*, 448. Nagarajan, V.; Fessenden, R. W. *Chem. Phys. Lett.* **1984**, *112*, 207; *J. Phys. Chem.* **1985**, *89*, 2330; **1989**, *93*, 6095 and references therein. See also refs 22 and 26.

0002-7863/90/1512-1277$02.50/0